Scientia Iranica B (2015) 22(3), 804–812

SCIENTIA IRANICA

Sharif University of Technology
Scientia Iranica
Transactions B: Mechanical Engineering
www.scientiairanica.com

A new theoretical analysis for the splitting of square columns subjected to axial loading

A. Niknejad* **and S. Bonakdar**

Department of Mechanical Engineering, Faculty of Engineering, Yasouj University, Yasouj, P.O. Box 75914-353, Iran.

Received 19 December 2012; received in revised form 7 August 2014; accepted 22 September 2014

KEYWORDS
Axial load;
Crack propagation;
Energy absorption;
Splitting;
Square column.

Abstract. In this article, some theoretical relations are derived to predict instantaneous axial load during the splitting process of square columns on rigid pyramidal dies. For this purpose, it is assumed that kinetic energy is dissipated by four different deformation mechanisms: bending, friction, crack propagation and expansion. These mechanisms are carefully assessed. Based on the principle of energy conservation, the external work of axial force is equated with total dissipated energies during the plastic deformation, and final relations are obtained to predict the load-displacement diagram. Also, the curl radius of square columns during the splitting process is calculated theoretically. Then, some metal tubes are tested and compressed axially between a rigid plate and a pyramidal die. Cracks propagate along four corners of the column. Experiments show that all four free end sides roll up into curls with a constant radius, and applied load becomes constant after crack propagation. This mechanism results in a large stroke and a constant load. Therefore, splitting is introduced as an energy absorber mechanism with large stroke to length ratio and high specific absorbed energy. Comparison of the theoretical predictions by derived equations, with the experimental results, shows good correlation.

1. Introduction

Thin-walled tubes and columns are widely used as structural components in industrial applications due to their excellent load-carrying capacity and energy absorption characteristics [1]. When thin-walled members are used as energy absorber elements under axial, lateral or bending loads, they show a variety of deformation modes, such as folding of circular simple [2] and grooved tubes [3], folding of square and rectangular columns [4], internal [5] and external tube inversion [6], flattening of circular [7] and square tubes [8], and indentation of circular [9] and rectangular tubes [10].

Energy absorber systems that are designed to limit impact forces in accident situations require a long stroke for application over a range of impact velocities. Tube splitting and curling are more efficient than transverse crushing, axial buckling and tube inversion and they have a better stroke to length ratio than these alternative deformation modes [11]. Stronge et al. [11] investigated the splitting process of square columns under axial loading using theoretical and experimental methods. They developed a theoretical model of the energy absorber system, based on static and impact tests on square, cross-sectional aluminum tubes. Reddy and Reid [12] introduced a novel mode of the deformation of circular tubes subjected to axial compression load during the splitting process. In their research, a number of axial cracks were produced in circular metal tubes and the strips formed and bent into curls. They found that the major part of the deformation takes place at a nearly constant load, which can be increased by preventing the formation of the curls. A simple upper bound approach was

*. *Corresponding author. Tel.: +98 74 33229889;*
Fax: +98 74 33221711
E-mail address: Aniknejad@yu.ac.ir (A. Niknejad)

used to estimate the operating load. Experimental results showed that the operating load of a splitted tube is somewhat lower than the corresponding value of the axial buckling and inversion mode. However, the maximum stroke of the splitting process is more than 90% of the tube length; therefore, the total absorbed energy by the splitting process is often as well as the axial buckling and inversion mode [12]. Niknejad et al. [13] analyzed splitting process of circular metal tubes by theoretical and experimental methods and calculated an analytical relation for predicting the curl radius of the tubes during the process. Also, Yuen et al. [14] investigated the splitting process of circular tubes under blast load, using a cutting die.

Lu et al. [15] performed an experimental investigation to study tearing energy in the splitting process of square aluminum and mild steel tubes. With little friction coefficient, and pre-cutting corners to different lengths, the plastic bending and tearing energies have been well estimated. A simple empirical formula was obtained to predict the tearing energy of the process.

Review of previously published work reveals that the splitting mode of deformation is a special case of tube inversion, where the die radius is large enough to cause splitting instead of inversion [16]. Huang et al. [17] investigated energy absorption by the splitting process in square columns under quasi-static loading. The metal tube was compressed axially between a plate and a pyramidal die. Experiments showed that the applied load became constant after the initial peak load initiated the cracks. Also, they studied the axial splitting and curling behavior of circular metal tubes using theoretical and experimental methods. Mild steel and aluminum circular tubes were pressed axially into a series of conical dies; each with a different semi-angle. An approximate analysis was presented, which successfully predicted the number of propagated cracks, the curling radius and the force applied. Effects of tube dimensions, semi-angle of the die, and friction were discussed in detail [18]. Previous research shows that the splitting of tubes is a function of die radius and frictional effects. Therefore, these parameters can be modified to achieve a desired rectangular shaped force-deflection, which is ideal for the design of energy absorbers [19].

This paper presents a new theoretical analysis, based on the energy method, to investigate energy absorption by square metal columns during the splitting process. Metal columns are compressed axially into a pyramidal die. To prevent buckling effects, each corner of the columns has an initial saw cut. These cracks propagate along the corners and side wall curls with a constant radius. Then, some experimental tests are performed on the square brazen and aluminum columns to verify the theoretical formula of the instantaneous splitting force.

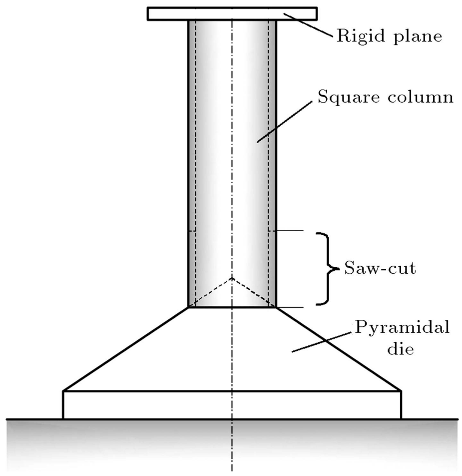

Figure 1. Schematic picture of the experimental set-up.

Figure 2. Two different specimens after the test.

2. Theoretical analysis

Figure 1 shows the experimental set-up of the splitting process on square metal columns. The pyramidal die is fixed to the bottom of the testing machine and a hard metal plane as a rigid body is placed over the column to make the load steady. The axes of the die, the column and the testing machine are carefully coincident. An initial saw-cut for all specimens is made in each corner to prevent buckling and to establish the split and curl mode. The cross-head of the testing machine forces the column down against the pyramidal die with a constant and low speed; therefore, the splitting process can be assumed a quasi-static process. Then, the created cracks propagate along each corner. Figure 2 shows two different specimens after the splitting tests.

Figure 3 shows a schematic diagram of axial force versus axial displacement during the splitting process on a square column. According to the mechanical behavior and deformation modes of the column during the process, and considering Figure 3, the splitting process is divided into four different stages, as a new theoretical deformation model:

Stage 1: OA; elastic deformation,

Stage 2: AB; plastic bending deformation,

Stage 3: BC; crack tip expansion,

Stage 4: CD; crack propagation and curling side walls.

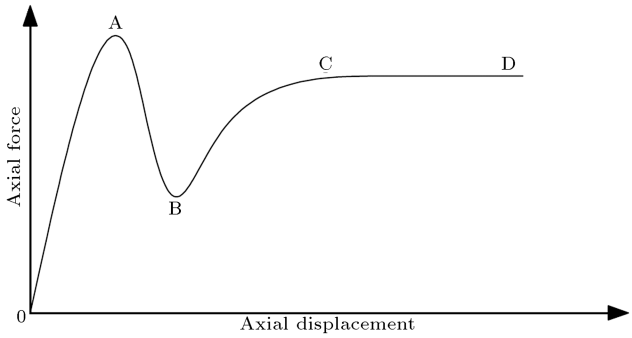

Figure 3. A schematic diagram of force displacement during the splitting process.

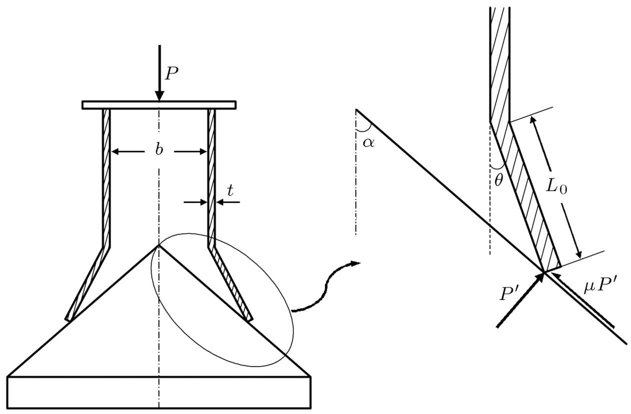

Figure 4. Deformation of a square column during the second stage of the new theoretical model.

The first stage is referred to as elastic deformation and the experimental tests show that the elastic part has a dispensable share of total axial displacement and absorbed energy by the column. Therefore, this article does not study the elastic stage.

In the second stage, as shows in Figure 4, axial force, P, bent the bottom part of the column with an initial length of L_0 around the end point of the initial saw-cut. In the third stage, each edge of the square column expands in a circumferential direction. In the fourth stage, crack propagation initiates and continues and, so, the axial force remains constant during the continuance of the splitting process.

In Stage 2, the sharp edges of the column move over the die, but, during the next stages, the smooth surface of the inner column walls is contacted to the die. Therefore, the friction coefficient of the splitting process in Stage 2 is bigger than the corresponding quantity in the third stage.

2.1. Second stage

Usually, in the splitting process, to prevent buckling and to establish the split and curl modes, an initial saw-cut with an initial length of L_0 is made in each corner of the column. During the second stage of the theoretical model, four plates of columns with length L_0 bend around four horizontal hinge lines, according to Figure 4. By considering the static equilibrium relations, the following relation is obtained:

$$P' = \frac{P}{4(\sin\alpha + \mu_1\cos\alpha)}, \tag{1}$$

where P' is the normal force to each side of the die surface; P is axial force subjected to the column; μ_1 is the friction coefficient between the sharp edges of the column and the die surface; and α indicates the semi angle of the pyramidal die. Therefore, the friction force of each column edge is calculated as:

$$F_f = \frac{\mu P}{4(\sin\alpha + \mu_1\cos\alpha)}. \tag{2}$$

Absorbed energy by the bending mode around the four horizontal hinge lines, with total length of $L = 4b$ from $\theta = 0$ to θ, is calculated as:

$$E_1 = \int_0^\theta M_0 L d\theta = 4M_0 b\theta, \tag{3}$$

where M_0 is the fully plastic bending moment and angle θ is shown in Figure 4. b indicates the square cross-section edge length. According to Figure 4, during the bending process of the second stage, angle θ increases from zero to the maximum value of α. The fully plastic bending moment is equal to:

$$M_0 = \frac{1}{4}\sigma_0 t^2, \tag{4}$$

where t is the wall thickness of the column cross-section, and σ_0 is the flow stress of the column material, calculated as follows [20]:

$$\sigma_0 = \sqrt{\frac{\sigma_u.\sigma_y}{1+n}}. \tag{5}$$

In the above equation, σ_u, σ_y and n are ultimate stress, yield stress and strain hardening exponent of the material, respectively. Axial displacement of a column during the second stage of the splitting process is indicated by Δ_1, and, based on geometrical relations, it is calculated as follows:

$$\Delta_1 = L_0\left[1 - \cos\theta + \frac{\sin\theta}{\tan\alpha}\right]. \tag{6}$$

Also, displacement of end edges of a square column in the direction of the die surface is obtained as:

$$\Delta_1' = L_0\sqrt{1 - \cos^2\theta + \frac{\sin^2\theta}{\tan^2\alpha}}. \tag{7}$$

Based on the energy method and the principle of the conservation of energy, the following relation is obtained as the governing equation of the splitting process on square columns:

$$P\Delta_1 = E_1 + F_f \Delta_1'. \tag{8}$$

Therefore, the axial force on a square column during the second stage of the splitting process is derived as:

$$P = \frac{\sigma_0 b t^2 \theta}{\Delta_1 - \frac{\mu_1 \Delta_1'}{4(\sin\alpha + \mu_1 \cos\alpha)}}, \qquad 0 \le \theta \le \alpha. \tag{9}$$

2.2. Third stage

When the end parts of the column with length L_0 bend around four horizontal hinge lines, and the value of angle θ reaches α, the third stage of the splitting process on the square column is started. On the other hand, in the third stage, the curling of the column walls is started and the perimeter of the cross-section of the square column increases. By considering the column as a rigid-perfectly plastic material, the total absorbed energy by a square column during the third stage of the splitting process (E_2) is calculated as:

$$E_2 = \sigma_0 . v . \sum_{i=1}^{j} \varepsilon_i, \tag{10}$$

where v is the volume of the column material and is assumed to remain constant. In the above equation, j is the number of assumed strains in the theoretical model of deformation during the third stage. The volume of the column material is equal to:

$$v = 4bt\Delta. \tag{11}$$

In the above equation, Δ is the axial displacement all over the splitting process. Also, the axial force subjected to the column during the third stage of the splitting process is equal to:

$$P = \frac{E_2}{\Delta}. \tag{12}$$

In the third stage of the theoretical model of deformation, two kinds of strain are considered: The strain of bending around the contact point of the column and die, and the strain of crack tip expansion. Bending strain is calculated as:

$$\varepsilon_1 = \frac{y}{\rho_0}. \tag{13}$$

In the above equation, y indicates the normal distance of an arbitrary point to neutral axes. According to Figure 5, the curvature radius of ρ_0 is determined as:

$$\rho_0 = R + t/2, \tag{14}$$

where R is the curl radius. By substituting Eq. (14) and $y = t/4$ in Eq. (13), the bending strain is obtained as:

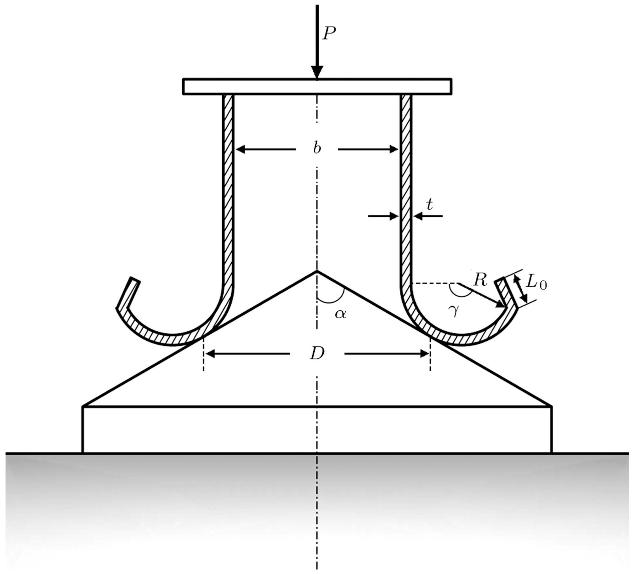

Figure 5. Deformation of a square column during the third stage of the new theoretical model.

$$\varepsilon_1 = \frac{t}{4R + 2t}. \tag{15}$$

The initial perimeter of the square cross-section is equal to:

$$H_1 = 4(b + t). \tag{16}$$

The perimeter of the square cross-section during the curling of the third stage is obtained as:

$$H_2 = 4(b + t) + 4(2R + t)(1 - \cos\gamma). \tag{17}$$

The circumferential strain of crack tip expansion is:

$$\varepsilon_2 = \frac{(2R + t)(1 - \cos\gamma)}{b + t}. \tag{18}$$

Angle γ is shown in Figure 5. By substituting Eqs. (15) and (18) into Eq. (10), the absorbed energy by bending and the crack tip expansion of the square column in the third stage is calculated as:

$$E_2 = 4(b+t)t\Delta\sigma_0 \left(\frac{t}{4R + 2t} + \frac{(2R+t)(1-\cos\gamma)}{b + t} \right). \tag{19}$$

In the above equation, the curl radius, R, is an unknown quantity and is calculated based on the minimum principle in plasticity:

$$\frac{\partial E_2}{\partial R} = 0. \tag{20}$$

Therefore, the curl radius is obtained as follows:

$$R = \frac{\sqrt{t(b + t)}}{4 \sin\frac{\alpha}{2}} - \frac{t}{2}. \tag{21}$$

The above relation is the first theoretical equation for predicting the curl radius during the splitting process on square columns.

Friction force in the third stage of the splitting process is calculated as the previous stage. In the third stage, axial displacement of the square column is equal to the movement of column walls over the pyramidal die. Therefore, the governing Eq. (8) is rewritten as the following:

$$P\Delta = E_2 + F_f\Delta. \tag{22}$$

In the above equation, Δ indicates axial displacement of the splitting process. In the third stage, the friction force is applied to smooth surface of the inner wall of the square column and, therefore, the friction coefficient of the third stage (μ_2) is less than the corresponding parameter of the second stage (μ_1). Axial force during the third stage of the splitting process is determined as below:

$$P = \frac{4(b+t)t\sigma_0\left[\frac{t}{4R+2t} + \frac{(2R+t)}{(b+t)}(1-\cos\gamma)\right]}{1 - \frac{\mu_2}{4(\sin\alpha + \mu_2\cos\alpha)}},$$

$$0 \leq \gamma \leq \gamma_{th}. \tag{23}$$

In the above equation, when $\gamma = \gamma_{th}$, in the four corners of the column, cracks start to propagate. As shown in Figure 5, angle γ increases from zero to the maximum value at which crack propagation is started (γ_{th}). The axial displacement of the column during the third stage of the splitting process is derived as:

$$\Delta_2 = L_0 + R\gamma. \tag{24}$$

2.3. Fourth stage

In this stage, cracks propagate along the four corners of the square column. According to Figure 6, the density of strain energy due to crack propagation is equal to the area under the stress-strain diagram of the material. Moreover, the friction force and bending of the curls dissipate the energy during the fourth stage. To determine dissipated energy by crack propagation, the material behavior of metal columns is assumed as elastic-plastic, with linear work hardening, as shown in Figure 6. Calculation of the area under the lines, OA and AB, results in the density of the absorbed energy by crack propagation:

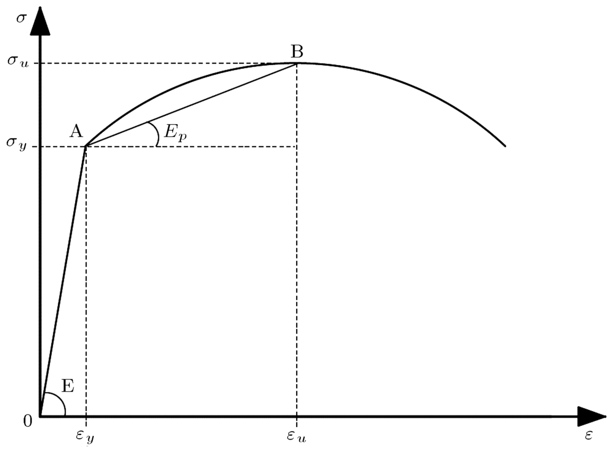

Figure 6. A schematic stress-strain diagram of a ductile material.

$$E_c = \frac{\sigma_y^2}{2E} + \frac{\sigma_y + \sigma_u}{2}\left(\varepsilon_u - \frac{\sigma_y}{E}\right). \tag{25}$$

In the above equation, E and ε_u indicate elasticity modulus and ultimate strain of column material, respectively. According to Figure 6, ultimate strain (ε_u) is estimated as follows:

$$\varepsilon_u = \frac{\sigma_u}{E_p} - \frac{\sigma_y}{E_p}\left(1 - \frac{E_p}{E}\right). \tag{26}$$

where E_p is the proportional modulus of the plastic zone. Substituting the above equation in Eq. (25) results in the dissipated energy due to four crack propagations:

$$E_{4c} = 4E_c = \frac{2\sigma_y^2}{E} + \frac{2(\sigma_u^2 - \sigma_y^2)}{E_p}. \tag{27}$$

According to the theoretical model of deformation, the cracks start to propagate, when:

$$\varepsilon_u = \varepsilon_2. \tag{28}$$

By substituting Eqs. (18) and (26) in Eq. (28), the threshold angle, γ_{th}, corresponding to the starting point of crack propagation, is calculated as follows:

$$\gamma_{th} = \cos^{-1}\left[1 - \frac{b+t}{2R+t}\left(\frac{\sigma_u}{E_p} - \frac{\sigma_y}{E_p} + \frac{\sigma_y}{E}\right)\right]. \tag{29}$$

According to the present theoretical model, in the third stage, when $\gamma = \gamma_{th}$, the cracks start to propagate. The fourth stage starts and, also, the axial force remains constant. Therefore, the axial force of the fourth stage of the splitting process on a square column is derived as:

$$P = \frac{4(b+t)t\sigma_0\left[\frac{t}{4R+2t} + \frac{(2R+t)}{(b+t)}(1-\cos\gamma_{th})\right]}{1 - \frac{\mu_2}{4(\sin\alpha + \mu_2\cos\alpha)}},$$

$$\gamma \geq \gamma_{th}. \tag{30}$$

3. Experiment

All experiments were performed by a DMG testing machine. The cross-head of the testing machine forced the square column slowly downward, with a constant rate of 20 mm/min, against the pyramidal die. The

Table 1. Geometrical dimensions of the different specimens.

Specimen code	Specimen material	External dimensions (mm×mm)	Wall thickness (mm)	Length of saw-cut (mm)	Length of column (mm)
BR01	Brass	35 × 35	1.0	5.0	99.2
BR02	Brass	40 × 40	1.0	5.0	80.5
BR03	Brass	50 × 50	1.0	5.0	78.9
AL01	Aluminum	35 × 35	1.7	7.0	70.6
AL02	Aluminum	45 × 45	1.9	7.0	70.8

testing machine illustrates the applied force, P, versus the axial displacement of the square column.

The pyramid semi-angle (α) of the die was selected equal to 75°. The die is made from hardened steel. Table 1 gives the geometrical dimensions of the different specimens. Three different geometrical groups of brazen columns and two different groups of aluminum columns were prepared to study the material effects of square columns on theoretical predictions by the presented formulas. Also, the same three specimens of each group were axially compressed under the same test conditions to investigate the repeatability of the splitting tests. According to standard ASTM E8M, a dumbbell shaped specimen of each column material was prepared and used in the quasi-static tensile tests to determine the material properties of the square columns. Figure 7 shows the quasi-static normal stress of a dumbbell shaped specimen of the aluminum square column, with an external cross-section of 35 mm×35 mm, versus the axial strain. Table 2 gives the material properties of the different square columns.

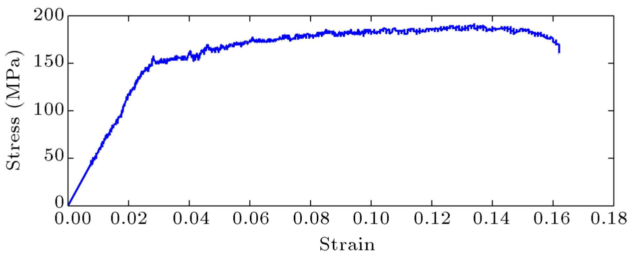

Figure 7. Stress-strain diagram of the aluminum square column with the external dimension of 35 × 35.

The experiments show that when the axial compression test is started, the initial saw-cuts at four corners cause the square column to divide into four plates. After that, curling is started and all four plates bend outwards into rolls.

4. Results and discussion

This article studies the splitting process of square columns and introduces some theoretical formulas to predict the diagram of instantaneous axial force versus axial displacement during the process. For this purpose, a new theoretical model of deformation was introduced that divides the splitting process into four different stages. In the first stage, the linear elastic deformation occurs in the column. Then, in the second stage, the bending around four hinge lines is modeled, theoretically. In the third stage, expansion of the cracks tips is studied. Finally, the steady axial force of the fourth stage was derived. Figures 8 and 9 compare the predicted diagram by the present theoretical analysis with the corresponding experimental curves of the axial force versus axial displacement during the splitting process on square aluminum specimens, AL01 and AL02, respectively. An initial 7.0 mm saw-cut was made in each corner of the aluminum columns. All the experimental tests were carried out using a pyramidal die with a semi-angle of $\alpha = 75°$. Comparison of the experimental curve with the theoretical prediction in Figures 8 and 9 affirms that the theoretical analysis and the final relations for predicting the axial force-displacement diagram during the splitting process on the square aluminum columns

Table 2. Material properties of the different square columns.

Columns material	External dimensions (mm×mm)	Flow stress (MPa)	Yield stress (MPa)	Ultimate stress (MPa)	Elasticity modulus (GPa)	Plastic modulus, E_p (GPa)
Aluminum	35 × 35	156	150	190	70	3.80
Aluminum	45 × 45	168	154	212	70	7.96
Brass	35 × 35	302.78	307	447.92	110	24.29
Brass	40 × 40	262.69	260	396.28	110	3.78
Brass	50 × 50	262.69	260	396.28	110	3.78

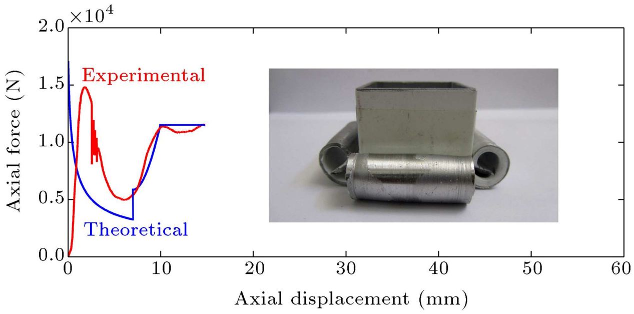

Figure 8. Comparison of the theoretical and experimental diagrams of an aluminum square column with the external dimension of 35 × 35.

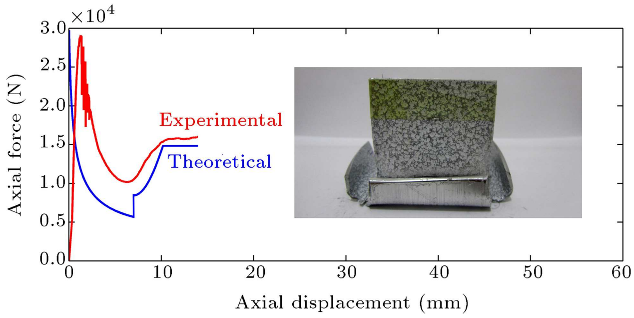

Figure 9. Comparison of the theoretical and experimental diagrams of an aluminum square column with the external dimension of 45 × 45.

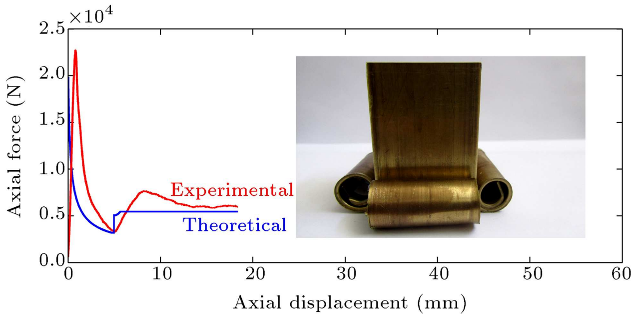

Figure 10. Comparison of the theoretical and experimental diagrams of a brazen square column with the external dimension of 35 × 35.

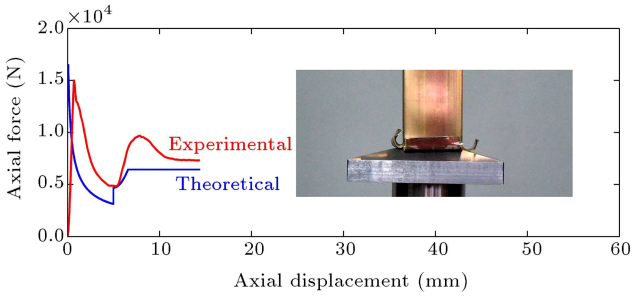

Figure 11. Comparison of the theoretical and experimental diagrams of a brazen square column with the external dimension of 40 × 40.

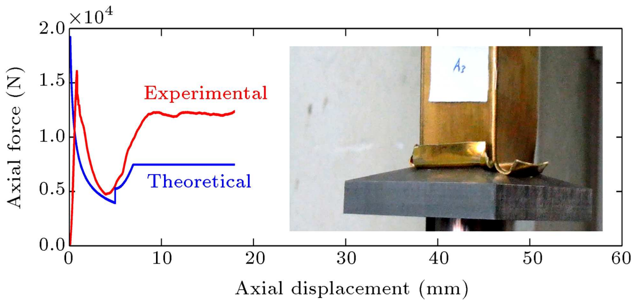

Figure 12. Comparison of the theoretical and experimental diagrams of a brazen square column with the external dimension of 50 × 50.

have a reasonable correlation with experiments. It shows the precision and accuracy of the theoretical equations. Also, the figures show that the theoretical analysis estimates the steady axial force of the splitting process with good agreement, compared with experimental measurements. It shows that the assumption of material behavior as the elastic-plastic with linear work hardening is suitable and compatible with the physical performance of the column materials. Also, a good correlation of the start point of crack propagation in both theoretical and experimental diagrams, results in the initial assumption for predicting the start point of crack propagation (Eq. (28)) to be correct. Although, the present analysis of the fourth stage is simpler than fracture mechanics theories; the analytical Eq. (30) can predict the axial force and the start point of crack propagation with acceptable correlation.

Figures 10-12 show experimental and theoretical diagrams of axial force versus axial displacement during the splitting process on the square brazen columns with different geometrical dimensions and material properties.

Comparison between theoretical and experimental diagrams of the brazen columns shows that the theoretical predictions by the derived equations in this article can predict variations of axial force during the splitting process with logical error. Also, a reasonable agreement between the slopes of both the corresponding curves of the second stage shows that the general form of the final formulas is correct and the derived relations can predict the physical behavior of the column and plastic deformations during the splitting process.

Reviewing the performed comparison in Figures 8-12 results in the theoretical analysis estimating the load-displacement diagram of the splitting process of square columns with satisfactory agreement, independent of column material type. However, there are some differences between some parts of the theoretical and experimental curves. Performed comparisons show that, in most cases, the third and fourth stages of the experimental results are estimated by the present theoretical analysis with good agreement, but, there are some considerable differences between each pair of curves in the second stage. In the derived theoretical analysis, two kinetic energy absorber mechanisms of plastic bending and friction were considered for the second stage of the analytical deformation model. The mentioned differences in the second stage of theoretical and experimental curves indicate that there are some other energy dissipater mechanisms in the second stage. If these unknown mechanisms are considered in the theory, estimations by the theoretical relations of the second stage improve. Furthermore, Figures 8-12 show that the differences between the second stage of the theoretical and experimental curves are larger for aluminum columns, compared with the brazen specimens, and shows that the accuracy of the theoretical predictions of the second stage for the brazen samples is more acceptable. Also, Eqs. (9), (23) and (30) conclude that increments of column wall thickness have more effect on energy absorption capability by the structure during the splitting process, with respect to increments of column edge length.

Huang et al. [17] obtained the following empirical relation to predict the curl radius of square metal columns during the splitting process, from the best fitted line of their test values:

$$R = \frac{32.7}{\sin\alpha} - 25.7. \tag{31}$$

Based on theoretical analysis, the present article introduced Eq. (21) to estimate the curl radius of square metal columns during the splitting process. The suggested Eq. (21) predicts the curl radius versus wall thickness and edge length of the column cross-section and semi angle of the pyramidal die. But, the suggested formula by Huang et al. [17] (Eq. (31)) only calculates the curl radius versus the semi angle of the pyramidal die. On the other hand, according to Huang's equation, the curl radius of the square columns during the splitting process is independent of the geometrical dimensions of the column. But, experimental results of the present article and previous work show that the curl radiuses of different square columns, with different wall thicknesses and cross-section edge lengths, and the same material, on the same pyramidal die, are not the same. Therefore, experimental results show that the curl radius of square columns during the splitting process is dependent on column wall thickness and each edge length of the square cross-section. It shows that theoretical Eq. (21), which was calculated in the present article, has better correlation with experimental results than the predictions by empirical Eq. (31) that was introduced in Ref. [17]. For example, the experimental curl radius of the square aluminum specimen, AL01, was measured equal to 2.4 mm. The empirical Eq. (31) predicts the curl radius of specimen AL01 equal to 8.154 mm and the obtained error percentage is 239%. But, theoretical Eq. (21) estimates the corresponding value equal to 2.394 mm, which shows that the error percentage is less than 1%. Also, the experimental curl radius of the square aluminum specimen, AL02, is 2.7 mm, and corresponding predictions by Eqs. (31) and (21) are 8.154 and 2.927 mm, respectively. The results show that the error percentages by Huang's and the present article's formula are 262 and 8.4%, respectively.

Therefore, Eq. (21) as the first theoretical equation for predicting the curl radius of square columns during the splitting process has good agreement, compared with experimental results.

5. Conclusion

In this article, some theoretical relations are derived to predict axial force during the splitting process on square columns. For this purpose, a new theoretical model of deformation is introduced that divides the splitting process into four different stages. In the first stage, the linear elastic deformation occurs in the column. Then, in the second stage, the bending around four hinge lines is considered in the specimens. In the third stage, expansion occurs at the crack tip; therefore, all four cracks propagate along the corners. Also, in this study, the curl radius is calculated theoretically. Finally, predictions of the theoretical relations are compared with experimental results, which show good agreement.

References

1. Zhang, X., Cheng, G. and Zhang, H. "Numerical investigations on a new type of energy-absorbing structure based on free inversion of tubes", *Int. J. Mech. Sci.*, **51**, pp. 64-76 (2009).

2. Bardi, F.C., Yun, H.D. and Kyriakides, S. "On the axisymmetric progressive crushing of circular tubes under axial compression", *Int. J. Solid. Struct.*, **40**, pp. 3137-3155 (2003).

3. Niknejad, A., Abedi, M.M., Liaghat, G.H. and Zamani Nejad, M. "Prediction of the mean folding force during the axial compression in foam-filled grooved tubes by theoretical analysis", *Mater. Des.*, **37**, pp. 144-151 (2012).

4. Niknejad, A., Liaghat, G.H., Moslemi Naeini, H. and Behravesh, A.H. "Experimental and theoretical investigation of the first fold creation in thin walled columns", *Acta Mech. Solida Sin.*, **23**(4), pp. 353-360 (2010).

5. Rosa, P.A., Rodrigues, J.M.C. and Martins, P.A.F. "Internal inversion of thin-walled tubes using a die: Experimental and theoretical investigation", *Int. J. Mach. Tool. Manuf.*, **44**, pp. 775-784 (2004).

6. Niknejad, A. and Moeinifard, M. "Theoretical and experimental studies of the external inversion process in the circular metal tubes", *Mater. Des.*, **40**, pp. 324-330 (2012).
7. Niknejad, A., Elahi, S.A. and Liaghat, G.H. "Experimental investigation on the lateral compression in the foam-filled circular tubes", *Mater. Des.*, **36**, pp. 24-34 (2012).
8. Gupta, N.K. and Khullar, A. "Collapse load analysis of square and rectangular tubes subjected to transverse in-plane loading", *Thin-Walled Struct.*, **21**, pp. 345-358 (1995).
9. Elchalakani, M., Zhao, X.L. and Grzebieta, R.H. "Plastic mechanism analysis of circular tubes under pure bending", *Int. J. Mech. Sci.*, **44**, pp. 1117-1143 (2002).
10. Kim, T.H. and Reid, S.R. "Bending collapse of thin-walled rectangular section columns", *Comput. Struct.*, **79**, pp. 1897-1911 (2001).
11. Stronge, W.J., Yu, T.X. and Johnson, W. "Long stroke energy dissipation in splitting tubes", *Int. J. Mech. Sci.*, **25**(9-10), pp. 637-647 (1983).
12. Reddy, T.Y. and Reid, S.R. "Axial splitting of circular metal tubes", *Int. J. Mech. Sci.*, **28**(2), pp. 111-131 (1986).
13. Niknejad, A., Rezaei, B. and Liaghat, G.H. "Empty circular metal tubes in the slitting process-theoretical and experimental studies", *Thin-Walled Struct.*, **72**, pp. 48-60 (2013).
14. Chun Kim Yuen, S., Altenhof, W., Opperman, C.J. and Nurick, G.N. "Axial splitting of circular tubes by means of blast load", *Int. J. Impact Eng.*, **53**, pp. 17-28 (2013).
15. Lu, G., Ong, L.S., Wang, B. and Ng, H.W. "An experimental study on tearing energy in splitting square metal tubes", *Int. J. Mech. Sci.*, **36**(12), pp. 1087-1097 (1994).
16. Alghamdi, A.A.A. "Collapsible impact energy absorbers: An overview", *Thin-Walled Struct.*, **39**, pp. 189-213 (2001).
17. Huang, X., Lu, G. and Yu, T.X. "Energy absorption in splitting square metal tubes", *Thin-Walled Struct.*, **40**, pp. 153-165 (2002).
18. Huang, X., Lu, G. and Yu, T.X. "On the axial splitting and curling of circular metal tubes", *Int. J. Mech. Sci.*, **44**, pp. 2369-2391 (2002).
19. Olabi, A.G., Morris, E. and Hashmi, M.S.J. "Metallic tube type energy absorbers: A synopsis", *Thin-Walled Struct.*, **45**, pp. 706-726 (2007).
20. Santosa, S. and Wierzbicki, T. "Crash behavior of box columns filled with aluminum honeycomb or foam", *Comput. Struct.*, **68**, pp. 343-67 (1998).

Biographies

Abbas Niknejad obtained his undergraduate degree in the area of Mechanical Engineering, in 2000, from Iran University of Science and Technology (IUST), Tehran, Iran. He received his post graduate degree in the area of Fracture Mechanics, in 2003, from Tarbiat Modares University (TMU), Tehran, Iran, from where he also received his PhD degree in the area of "Investigation of impact resistance and energy absorption ability by honeycomb structures with foam-filled cells". He is currently Assistant Professor in Mechanical Engineering-Applied Design, in the Mechanical Engineering Department at Yasouj University, Yasouj, Iran. Since 2010, he has supervised 8 MS degree projects and 4 projects as advisor and has had 16 articles published and 44 papers presented in international journals and at conferences. He joined the Iranian Society of Mechanical Engineers (ISME), in 2008. His research interests include experimental, theoretical and numerical analysis on plastic deformation, impact loadings, metal forming, and composite structures.

Saeed Bonakdar received his undergraduate degree, in 2012, from Yasouj University, Yasouj, Iran, in the area of "Theoretical and experimental studies on energy absorption capability of square metal columns during the axial splitting process", and is currently an MS degree scholar in Mechanical Engineering-Applied Design, in the Mechanical Engineering Department at the Petroleum University of Technology, Ahvaz, Iran. He has presented one article at an international conference.